UNLV | UNIVERSITY LIBRARIES

Electrical and Computer Engineering Faculty Publications

Electrical & Computer Engineering

2-11-2021

Generalized Composite Noncertainty-Equivalence Adaptive Control of a Prototypical Wing Section With Torsional Nonlinearity

Keum W. Lee
Catholic Kwandong University

Sahjendra N. Singh
University of Nevada, Las Vegas, sahjendra.singh@unlv.edu

Follow this and additional works at: https://digitalscholarship.unlv.edu/ece_fac_articles

 Part of the Controls and Control Theory Commons

Repository Citation

Lee, K., Singh, S. (2021). Generalized Composite Noncertainty-Equivalence Adaptive Control of a Prototypical Wing Section With Torsional Nonlinearity. *Nonlinear Dynamics, 103* 2547-2561.
http://dx.doi.org/10.1007/s11071-021-06227-3

This Article is protected by copyright and/or related rights. It has been brought to you by Digital Scholarship@UNLV with permission from the rights-holder(s). You are free to use this Article in any way that is permitted by the copyright and related rights legislation that applies to your use. For other uses you need to obtain permission from the rights-holder(s) directly, unless additional rights are indicated by a Creative Commons license in the record and/or on the work itself.

This Article has been accepted for inclusion in Electrical and Computer Engineering Faculty Publications by an authorized administrator of Digital Scholarship@UNLV. For more information, please contact digitalscholarship@unlv.edu.

Generalized Composite Noncertainty-Equivalence Adaptive Control of a Prototypical Wing Section with Torsional Nonlinearity

Keum W. Lee*

Catholic Kwandong University, Gangneung-si, Gangwon-do 25601, Republic of Korea

and

Sahjendra N. Singh†

University of Nevada Las Vegas, Las Vegas, NV 89154

Revised December 8, 2020

Abstract

The paper presents a generalized composite noncertainty-equivalence adaptive control system for the control of a prototypical aeroelastic wing section using a single trailing-edge control surface. The plunge-pitch (two-degree-of-freedom) dynamics of this aeroelastic system include torsional pitch-axis nonlinearity. The open-loop system exhibits limit cycle oscillations beyond a critical free-stream velocity. It is assumed that parameters of the model are not known. The objective is to suppress the oscillatory

*Professor, Department of Electronic Engineering, kwlee@cku.ac.kr, member AIAA

†Professor, Department of Electrical and Computer Engineering, sahaj@ee.unlv.edu

responses of the system. Based on the immersion and invariance approach, a generalized composite noncertainty-equivalence adaptive (NCEA) control system for regulation of the pitch angle is designed. The control system consists of a control module and a composite parameter identifier - designed independently. The composite integral parameter estimation law is based on (i) the immersion and invariance (I&I) theory, (ii) gradient-based adaptation algorithm, and (iii) classical certainty-equivalence adaptive (CEA) update rule. Besides the composite integral component, the full parameter estimate also includes a judiciously chosen nonlinear algebraic function. This composite identifier inherits stronger stability properties. Using the Lyapunov analysis, asymptotic suppression of the limit cycle oscillations and the boundedness of system trajectories are established. Interestingly, in the closed-loop system including the composite update rule, there exist two attractive manifolds to which the system's trajectories converge. Simulation results are presented which show the suppression of the oscillatory plunge displacement and pitch angle responses despite uncertainties in the model parameters. Furthermore, the performance and stability properties of this composite NCEA control system - including the gradient-based adaptation and the update rule of the CEA system - are better than the simple NCEA system.

Keywords Aeroelastic system . Composite adaptive control . Immersion and invariance . Noncertainty-equivalence adaptive control . Identifier . Limit cycle oscillation . Nonlinear adaptive control

Nomenclature

a	=	nondimensionalized distance from the midchord to the elastic axis
b	=	semichord of the wing
c_h	=	structural damping coefficient in plunge due to viscous damping
c_α	=	structural damping coefficient in pitch due to viscous

		damping
$k_1, (\gamma_g, \Gamma)$	=	feedback gain, adaptation gains
h	=	plunge displacement
I_α	=	mass moment of inertia of the wing about the elastic axis
k_h	=	structural spring constant in plunge
k_{α_i}	=	structural spring constants in pitch
m_t	=	mass of the plunge-pitch system
m_w	=	mass of the wing
M_s, M_d, B_0, g_0, b_0	=	system matrices
M, L	=	moment and lift
s_p, s	=	span, $\dot{\tilde{\alpha}} + \lambda_1 \tilde{\alpha}$
U, u	=	free-stream velocity and flap deflection
V_g, V_c	=	Lyapunov functions
x	=	state vector $(h, \alpha, \dot{h}, \dot{\alpha})^T$
x_α	=	nondimensionalized distance measured from the elastic axis to the center of mass
z	=	parameter error $\hat{\theta} - \theta$
α, α_r, $\tilde{\alpha}$	=	pitch angle, reference angle, $\alpha - \alpha_r$
β, β_f	=	flap deflection angle, filtered β
(ϕ, W), ϕ_f	=	regressor vectors, filtered ϕ
λ_1, (λ_f, k_f)	=	gain in s, filter parameters
μ	=	algebraic component of $\hat{\theta}$
ρ	=	density of air
θ	=	unknown parameter vector
$\hat{\theta}$, $\hat{\theta}_{Igc}$	=	estimate of θ, integral part of $\hat{\theta}$

1 Introduction

Aeroelastic systems can exhibit complex behavior, including multiple equilibria, divergence, limit cycle oscillations (LCOs), resonance, and even chaos [1-5]. These undesirable phenomena have adverse effect on the maneuverability of aircraft as well as on the flight envelope. For these reasons, researchers have focused on the design of active control systems for preserving stability in aeroelastic systems. For a benchmark active control technology (BACT) wind-tunnel model, constructed at the NASA Langley Research Center, researchers developed control algorithms for flutter suppression based on classical, minmax, passivity, robust, neural, and adaptive control techniques, as well as a gain scheduling method [6-11]. The authors of [12] developed a methodology by combining numerical continuation, harmonic balance, and multiobjective optimization techniques for the design of a control law to eliminate LCOs [12].

For a two-degree-of-freedom aeroelastic laboratory model at Texas A&M University, researchers examined the existence of LCOs in wind-tunnel tests and designed control systems using linear and feedback linearization control techniques [13-16]. Additionally, for the quasi-steady model of [13] with parametric uncertainties, adaptive laws have been designed [17-22]. The authors of [23] designed an adaptive control law for the choice of the plunge displacement as a controlled output variable for an unsteady aeroelastic system. A robust control system has also been designed in Ref. [24]. The authors of [25] proposed a terminal sliding mode control law for the suppression of LCOs of an aeroelastic system. The derivation of the adaptive laws of [17-23] is based on the certainty-equivalence principle [26]. Astolfi et al. [27] developed a methodology based on the notion of immersion and invariance (I&I) for the design of noncertainty-equivalence adaptive (NCEA) control laws. For avoiding the complexity in the design of [27], the authors of [28] used filtered signals for synthesis. Later, NCEA laws were designed for the control of aeroelastic systems [29-31].

In the past, with an aim to enhance the performance of certainty-equivalence adap-

tive (CEA) control systems, researchers proposed composite adaptive laws [32-35]. The identifier of these composite adaptive control systems use both the tracking error and model output error in the adaptation law. The combination of these two error signals provides distinct information about the parameter estimation error to the identifier. Naturally, composite (CEA) control laws achieve stronger stability properties in the closed-loop system, compared with CEA systems. It is well known that I&I-based NCEA laws yield improved performance, compared with CEA systems. Recently, composite NCEA control laws for a system formed by a chain of integrators with known control input coefficient [36] and for an asteroid-orbiting spacecraft [37] have been designed. The composite NCEA systems have stronger stability properties, compared with the NCEA systems. It appears from the literature that to date composite NCEA law has not been developed for aeroelastic systems.

The objective in this paper is to design a composite NCEA control system for the suppression of LCOs of a two degree-of-freedom quasi-steady aeroelastic model of Ref. [13], including torsional nonlinearity. A single trailing-edge flap is used for the purpose of control. It is assumed that all of the parameters (physical, aerodynamic, and the torsional stiffness) are unknown. The contribution of this paper is three-fold. First, for the pitch angle control, a generalized composite NCEA control law is derived. The controller consists of a control module and a composite identifier, which are designed independently. The adaptation law is formed by combining update laws of (i) the NCEA system, (ii) CEA system, and (iii) gradient based scheme. Of course, the full parameter estimate is formed by the output generated by the composite integral adaptation law and a judiciously selected nonlinear algebraic vector function. Second, the Lyapunov analysis shows that all of the signals are bounded and the pitch angle trajectory asymptotically converges to zero. Interestingly, the closed-loop control system including the composite parameter adaptation, has two attractive manifolds in an extended state space to which system trajectories converge. This does not happen in the NCEA or CEA

systems. Third, simulation results are presented. These results show that the composite NCEA law achieves suppression of the oscillatory plunge displacement and pitch angle LCOs despite uncertainties in the parameters. Furthermore, the performance and stability properties of the composite NCEA control system - including the gradient-based adaptation and the update rule of the CEA system - are better than the NCEA system.

It should be noted that the CEA laws of [17-23] and the NCEA laws of [29-31], designed for aeroelastic systems, have used the information only on the tracking error for parameter adaptation. But the generalized composite NCEA law developed here uses in addition model estimation error for the parameter adaptation. For this reason, the closed-loop system, including the composite NCEA law, has stronger stability properties. (Later, based on the Lyapunov analysis, additional stability properties of the generalized composite NCEA law compared with NCEA and CEA laws are discussed in Remark 2 and Remark 3, and Table 2 provides the response characteristics.)

The organization of the paper is as follows: Section 2 presents the aeroelastic model and a control module is designed in Section 3. This is followed by the design of a composite identifier and the analysis of closed-loop stability properties in Section 4. Finally, Section 5 presents the simulation results.

2 Aeroelastic Model and Control Problem

The geometry of the wing section with a trailing-edge control surface is shown in Fig. 1. A laboratory model of this wing section has been developed at the Texas A&M University for the evaluation of performance of control laws [13, 15]. Its two-degree-of-freedom plunge and pitch dynamics are governed by the following second-order differential equations [13]:

$$\begin{bmatrix} m_t & m_w x_\alpha b \\ m_w x_\alpha b & I_\alpha \end{bmatrix} \begin{bmatrix} \ddot{h} \\ \ddot{\alpha} \end{bmatrix} + \begin{bmatrix} c_h & 0 \\ 0 & c_\alpha \end{bmatrix} \begin{bmatrix} \dot{h} \\ \dot{\alpha} \end{bmatrix}$$

$$+\begin{bmatrix} k_{h0} & 0 \\ 0 & k_\alpha(\alpha) \end{bmatrix}\begin{bmatrix} h \\ \alpha \end{bmatrix} = \begin{bmatrix} -L \\ M \end{bmatrix} \tag{1}$$

where h is the plunge displacement and α is the pitch angle. In equation (1), m_w is the mass of the wing; m_t is the total mass; b is the semichord of the wing; I_α is the moment of inertia; x_α is the nondimensionalized distance of the center of mass from the elastic axis; c_α and c_h are the pitch and plunge damping coefficients, respectively; and M and L are the aerodynamic moment and lift. The quasi-steady aerodynamic force (L) and moment (M), which act on the wing section, are given by

$$L = \rho U^2 b c_{l_\alpha} s_p \left[\alpha + \frac{\dot{h}}{U} + \left(\frac{1}{2} - a\right) b\frac{\dot{\alpha}}{U}\right] + \rho U^2 b c_{l_{\beta_f}} s_p \beta_f$$

$$M = \rho U^2 b^2 c_{m_\alpha} s_p \left[\alpha + \frac{\dot{h}}{U} + \left(\frac{1}{2} - a\right) b\frac{\dot{\alpha}}{U}\right] + \rho U^2 b^2 c_{m_{\beta_f}} s_p \beta_f \tag{2}$$

where a is the nondimensionalized distance from the midchord to the elastic axis, s_p is the span, c_{l_α} and c_{m_α} are the lift and moment coefficients per angle of attack, and $c_{l_{\beta_f}}$ and $c_{m_{\beta_f}}$ are lift and moment coefficients per trailing-edge flap deflection angle β. Although the design approach is applicable to models including higher-order linearly parameterized torsional nonlinearities, it is assumed that the stiffness function $k_\alpha(\alpha)$ is a polynomial in variable α of fourth degree of the following form:

$$k_\alpha(\alpha) = k_{\alpha_0} + k_{\alpha_1}\alpha + k_{\alpha_2}\alpha^2 + k_{\alpha_3}\alpha^3 + k_{\alpha_4}\alpha^4$$

Define the state vector as $x = (x_1, ..., x_4)^T = (\alpha, h, \dot{\alpha}, \dot{h})^T \in R^4$. Then a state space representation of equation (1) can be written as

$$\dot{x} = \begin{bmatrix} 0_{2\times2} & I_{2\times2} \\ M_s & M_d \end{bmatrix} x + \begin{bmatrix} 0_{2\times2} \\ g_0 \end{bmatrix} k_{n_\alpha} + \begin{bmatrix} 0_{2\times1} \\ b_0 \end{bmatrix} \beta$$
$$\doteq f(x) + B_0\beta \tag{3}$$

where $f(x)$ and B_0 are defined in Eq. (3), $\alpha k_\alpha = \alpha k_{\alpha_0} + k_{n_\alpha}$, and $k_{n_\alpha} = \alpha(k_{\alpha_1}\alpha + k_{\alpha_2}\alpha^2 + k_{\alpha_3}\alpha^3 + k_{\alpha_4}\alpha^4)$. The constant matrices M_s, M_d, $g_0 = [g_{01}, g_{02}]^T$, and $b_0 = (b_{01}, b_{02})^T$ can be obtained from Eq. (1).

For a fixed value of the parameter a, the stability of the open-loop model depends on the free-stream velocity U. For low velocities, the linearized system (3) with $\beta = 0$ has stable eigenvalues; therefore, the plunge and pitch angle trajectories beginning in the vicinity of the origin ($x = 0$) converge to zero. However, it is found that for $a = -0.6547$, beyond the critical velocity $U^* = 16.6750$ [m/s], the loci of the two complex eigenvalues of the linearized model cross into the right-half complex plane. Thus, treating U as a bifurcation parameter, the supercritical Andronov-Hopf bifurcation takes place and periodic orbits are born. The size of the limit cycle increases with U. For the model parameters of Refs. [13, 15] (also collected in the appendix for convenience), Fig. 2 shows the closed orbits in the phase planes $\alpha - \dot{\alpha}$ and $h - \dot{h}$ for two values of U. Clearly, the design of an active control law for the suppression of LCOs is necessary.

It is assumed that all the physical parameters of the wing section, as well as the aerodynamic lift and moment coefficients are unknown. This implies that the matrices M_s, M_d, g_0, and $k_{\alpha i}$ for $(i = 0, 1, ..., 4)$ are not known. Consider a smooth reference trajectory α_r tending to zero. The objective is to design a control law such that the tracking error $\tilde{\alpha} = \alpha - \alpha_r$ and the state vector asymptotically tend to zero despite uncertainties in the model parameters.

3 NCEA Pitch Angle Control Law

Next, the design of an immersion and invariance based generalized composite noncertainty-equivalence control law is considered. The control system has a modular structure - consisting of a control module and a composite parameter identifier. First, the design of a noncertainty-equivalence adaptive (NCEA) control module is considered. This will be followed by the design of a composite identifier. Here, the derivation of the control module is briefly presented for completeness. (The details of derivation can be found in Ref. [28].)

For the pitch angle trajectory control, the following assumption is made.

Assumption 1: It is assumed that the sign of the coefficient b_{01} of the control input β is known. However, its magnitude is assumed to be unknown.

Because the model has a single control surface for trajectory tracking control, the plunge displacement trajectory is not directly controlled. Therefore, the stability of the closed-loop system depends on zero dynamics. The zero dynamics are defined as the residual dynamics of the system, when the pitch angle is identically zero.

Assumption 2: It is assumed that the transfer function relating the input β and the output α of the linearized model about the origin has stable zeros. Thus, the zero dynamics have locally asymptotically stable equilibrium point.

For confirming the validity of Assumption 2, the zeros of the transfer function of the linearized model of the system were computed using model parameters in the appendix. The output α has relative degree two. Thus, the transfer function has two zeros. The three-dimensional plots in Fig. 3 show the real and positive imaginary parts of the complex conjugate zeros for a set of values of $U \in [10, 30]$ [m/s] and $a \in [-0.8, -0.4]$. It is seen that indeed, the model has stable zeros for the set of values of interest of (U, a). Because the zeros of the transfer function vary continuously as the system parameters change, zeros will remain stable for small variations in the other nominal model parameters as well.

For the pitch angle trajectory control, consider the second-order pitch angle dynamics obtained from Eq. (3) in a compact form as:

$$\ddot{\alpha} = \dot{x}_3 = \phi_a^T(x)\theta_a + b_1\beta \tag{4}$$

where $b_1 = sign(b_{01})b_{01} > 0$, the vector $\phi_a \in R^8$ is:

$$\phi_a(x) = (\alpha, h, \dot{\alpha}, \dot{h}, \alpha^2, \alpha^3, \alpha^4, \alpha^5)^T \in R^8$$

and $\theta_a \in R^8$ is a vector formed by the unknown constant coefficients.

It will be convenient to introduce a scalar function of the form:

$$s = \dot{\tilde{\alpha}} + \lambda_1 \tilde{\alpha}; \lambda_1 > 0 \tag{5}$$

Using Eq. (4), its derivative can be written as:

$$\dot{s} = \phi_a^T \theta_a + b_1 \beta - \ddot{\alpha}_r + \lambda_1 \dot{\tilde{\alpha}} \tag{6}$$

Adding and subtracting $k_1 s$ and factoring b_1, Eq. (6) can be expressed as:

$$\dot{s} = b_1[\phi_a^T b_1^{-1} \theta_a + b_1^{-1}(-\ddot{\alpha}_r + \lambda_1 \dot{\tilde{\alpha}} + k_1 s) + \beta] - k_1 s$$

$$\doteq b_1[\phi^T \theta + \beta] - k_1 s \tag{7}$$

where $k_1 > 0$ and:

$$\theta = [\theta_a^T b_1^{-1}, b_1^{-1}]^T \in R^9$$

$$\phi^T = [\phi_a^T, -\ddot{\alpha}_r + \lambda_1 \dot{\tilde{\alpha}} + k_1 s] \in R^9 \tag{8}$$

To this end, to avoid complexity in design using the original I&I theory, filtered signals s_f, ϕ_f, and β_f are generated using the following equations:

$$\dot{s}_f = -\lambda_f s_f + k_f s \tag{9}$$

$$\dot{\phi}_f = -\lambda_f \phi_f + k_f \phi \in R^9 \tag{10}$$

$$\dot{\beta}_f = -\lambda_f \beta_f + k_f \beta \tag{11}$$

where $\lambda_f > 0$ and $k_f > 0$. Essentially the signals s_f, ϕ_f, and β_f are the outputs of a filter transfer function:

$$H(p) = \frac{k_f}{p + \lambda_f}, k_f > 0, \lambda_f > 0 \tag{12}$$

with inputs s, ϕ, and β, respectively. Here, p denotes the Laplace variable or a derivative operator. (Note that Eq. (11) will not be implemented because later β_f is computed explicitly in Eq. (16)). Now filtering Eq. (7) using $H(p)$ gives:

$$\dot{s}_f = b_1[\phi_f^T \theta + \beta_f] - k_1 s_f \tag{13}$$

Let an estimate of θ be $\hat{\theta}$ where:

$$\hat{\theta} = \hat{\theta}_{Igc} + \mu \tag{14}$$

where the integral component $\hat{\theta}_{Igc}$ of $\hat{\theta}$ will be shown to satisfy a vector differential equation and μ will be obtained as an algebraic state-dependent vector function. This form of parameter estimate differs from parameter estimate of classical CEA control systems.

Define the parameter error as:

$$z = \hat{\theta} - \theta \tag{15}$$

In view of Eq. (13), one select an NCEA control law of the form:

$$\beta_f = -\phi_f^T \hat{\theta} = -\phi_f^T (\hat{\theta}_{Igc} + \mu) \tag{16}$$

Then, in the closed-loop system, one has:

$$\begin{aligned} \dot{s}_f &= b_1[\phi_f^T \theta - \phi_f^T \hat{\theta}] - k_1 s_f \\ &= -b_1 \phi_f^T z - k_1 s_f \end{aligned} \tag{17}$$

It follows from Eq. (17) that if $\phi_f^T z = 0$, then s_f converges exponentially to zero. Next, the design of a composite identifier will be considered.

4 Parameter Identifier

In this section, a composite parameter adaptation law, which is based on (i) the gradient algorithm-based adaptation scheme, (ii) I&I-based parameter adaptation rule, and (iii) a classical parameter update rule, is designed. First, the design of an update law based on the gradient algorithm is presented.

4.1 Gradient-Based Estimator Design

For design of the identifier, a static parametric model of the pitch-axis dynamics (Eq. (4)) will be useful. However, the signal $\dot{x}_3 = \ddot{\alpha}$ in Eq. (4) is not measured. Therefore, it is necessary to filter $\ddot{\alpha}$ using the first-order transfer function $H(p)$ given in Eq. (12). By filtering the signals in Eq. (4), one obtains:

$$H(p)\ddot{\alpha} = H(p)[\phi_a^T \theta_a + b_1 \beta] = \phi_{af}^T \theta_a + b_1 \beta_f \tag{18}$$

where:

$$\dot{\phi}_{af} = -\lambda_f \phi_{af} + \phi_a \tag{19}$$

Note that ϕ_a (see Eq. (8)) and ϕ_{af} are formed by the first eight elements of ϕ and ϕ_f, respectively. Thus:

$$H(p)\ddot{\alpha} = \frac{k_f p \dot{\alpha}}{p + \lambda_f} = k_f \dot{\alpha} - \frac{k_f \lambda_f \dot{\alpha}}{p + \lambda_f} \tag{20}$$

Also, one has:

$$\begin{aligned} \frac{k_f \lambda_f \dot{\alpha}}{p + \lambda_f} &= \frac{k_f \lambda_f (p + \lambda_f - \lambda_f)\alpha}{p + \lambda_f} \\ &= k_f \lambda_f \alpha - \frac{k_f \lambda_f^2 \alpha}{p + \lambda_f} \end{aligned} \tag{21}$$

Define:

$$\alpha_f = \frac{k_f \alpha}{p + \lambda_f} \tag{22}$$

Note that α_f is generated using the following differential equation:

$$\dot{\alpha}_f = -\lambda_f \alpha_f + k_f \alpha \tag{23}$$

Using Eq. (21) in (20) gives:

$$H(p)\ddot{\alpha} = k_f \dot{\alpha} - k_f \lambda_f \alpha + \lambda_f^2 \alpha_f \tag{24}$$

By dividing by b_1 in Eq. (18) and solving for β_f gives:

$$\beta_f = -\phi_{af}^T b_1^{-1} \theta_a + b_1^{-1} H(p)\ddot{\alpha} \tag{25}$$

Then, using Eq. (24), one obtains:

$$\beta_f = [-\phi_{af}^T, k_f \dot{\alpha} - k_f \lambda_f \alpha + \lambda_f^2 \alpha_f][b_1^{-1} \theta_a^T, b_1^{-1}]^T$$

$$\doteq W^T(\phi_f, \alpha, \dot{\alpha}, \alpha_f)\theta \tag{26}$$

where one has already defined parameter vector $\theta = [b_1^{-1}\theta_a^T, b_1^{-1}]^T$ and the regressor vector W is:

$$W = [-\phi_{af}^T, k_f\dot{\alpha} - k_f\lambda_f\alpha + \lambda_f^2\alpha_f]^T \in R^9 \tag{27}$$

For the derivation of an adaptation law, consider an estimation model [26]:

$$\hat{\beta}_f = W^T\hat{\theta} \tag{28}$$

where $\hat{\theta}$ is an estimate of θ. The parameter error is $z = \hat{\theta} - \theta$. Define the estimation error as:

$$e = \hat{\beta}_f - \beta_f \tag{29}$$

Using Eqs. (26) and (28) in Eq. (29) give the error e:

$$e = W^T\hat{\theta} - W^T\theta = W^T z \tag{30}$$

Next, for obtaining an update law, consider a performance index $J = (e^2/2)$ for minimization by the choice of $\hat{\theta}$. The gradient of J with respect to $\hat{\theta}$ is:

$$\frac{\partial J}{\partial \hat{\theta}} = e\frac{\partial e}{\partial \hat{\theta}} = We \tag{31}$$

Then, one chooses the parameter update law as [26]:

$$\dot{\hat{\theta}} = -\gamma_g We \tag{32}$$

where $\gamma_g > 0$ is an adaptation gain. Using Eq. (30), the derivative of the parameter error z can be expressed as:

$$\dot{z} = -\gamma_g We = -\gamma_g WW^T z \tag{33}$$

For analyzing the stability properties of the identifier, consider a Lyapunov function:

$$V_g = z^T z \tag{34}$$

Its derivative along the solution of Eq. (33) is:

$$\dot{V}_g = -2\gamma_g z^T W e = -2\gamma_g z^T W W^T z = -2\gamma_g e^2 \leq 0 \tag{35}$$

This implies that $z = 0$ is an stable equilibrium point of Eq. (33). Furthermore, integrating Eq. (35), it follows that e (i. e., $W^T z$) is a square integrable function. This completes the design of the gradient algorithm-based identifier.

4.2 Composition of Estimators Based on NCEA and CEA systems with Gradient Scheme

Next, a composite parameter identifier will be derived by combining the parameter adaptation laws of the NCEA and CEA systems, along with the gradient algorithm-based identifier. The parameter error is $z = \hat{\theta} - \theta = \hat{\theta}_{Igc} + \mu - \theta$. The algebraic part μ is selected as

$$\mu = \Gamma \phi_f s_f \tag{36}$$

where $\Gamma \in R^{9\times 9}$ is a positive definite symmetric matrix. For derivation of the integral adaptation law for $\hat{\theta}_{Igc}$, consider the dynamics of the parameter error z. The derivative of the parameter error vector z is:

$$\dot{z} = \dot{\hat{\theta}}_{Igc} + \dot{\mu} = \dot{\hat{\theta}}_{Igc} + \Gamma[\dot{\phi}_f s_f + \phi_f \dot{s}_f] \tag{37}$$

Substituting for $\dot{\phi}_f$ and $\dot{s}_f$ from Eqs. (10) and (17) in Eq. (37) gives:

$$\dot{z} = \dot{\hat{\theta}}_{Igc} + \Gamma[-\lambda_f \phi_f + k_f \phi] s_f + \Gamma \phi_f [-b_1 \phi_f^T z - k_1 s_f] \tag{38}$$

Similar to the I&I-based identifier design, the derivative of $\hat{\theta}_{Igc}$ is selected to cancel the known functions in Eq. (38). Additionally, the adaptation signal $-\gamma_g W e$ from Eq. (32) of the gradient-based estimator and a function $\gamma_c \phi_f s_f$ similar to CEA systems are included in $\dot{\hat{\theta}}_{Igc}$. In traditional CEA systems, the function $\gamma_c \phi_f s_f$ with $\gamma_c = 1$ forms the update law alone. The purpose of this function is to eliminate certain sign-indefinite function in the Lyapunov derivative to ensure stability in the system. Thus,

the composite integral adaptation law takes the form:

$$\dot{\hat{\theta}}_{Igc} = \Gamma[(\lambda_f \phi_f - k_f \phi) s_f + k_1 \phi_f s_f - \gamma_g W e + \gamma_c \phi_f s_f] \tag{39}$$

(Eq. (39) becomes an update law for an NCEA system if γ_g and γ_c are set to zero.) Substituting Eq. (39) in (38) gives:

$$\dot{z} = \Gamma[-b_1 \phi_f \phi_f^T z - \gamma_g W e + \gamma_c \phi_f s_f] \tag{40}$$

This completes the design of the composite identifier.

4.3 Closed-Loop System Stability Analysis

In this subsection, stability properties of the closed-loop system - including the control law (16) and the adaptation law (39) - are examined. Consider a Lyapunov function:

$$V_c(s_f, z) = \frac{s_f^T s_f}{2} + \frac{b_1}{2} z^T \Gamma^{-1} z \tag{41}$$

The derivative of V_c along the solution of the system Eqs. (17) and (40) is:

$$\dot{V}_c = s_f[-b_1 \phi_f^T z - k_1 s_f] + z^T \Gamma^{-1} \Gamma[-b_1^2 \phi_f \phi_f^T z - b_1 \gamma_g W e + b_1 \gamma_c \phi_f s_f] \tag{42}$$

Similar to CEA systems, the sign-indefinite function $-b_1 \phi_f^T z$ is eliminated by setting $\gamma_c = 1$. Then, Eq. (42) takes a simplified form given by:

$$\dot{V}_c = -k_1 s_f^2 - b_1^2 (\phi_f^T z)^2 - b_1 \gamma_g z^T W e \tag{43}$$

Because $e = W^T z$, one obtains:

$$\dot{V}_c = -k_1 s_f^2 - b_1^2 (\phi_f^T z)^2 - b_1 \gamma_g (W^T z)^2 \tag{44}$$

The Lyapunov function $V_c(s_f, z)$ is a positive definite function of s_f and z, and $\dot{V}_c \leq 0$. Thus, $V_c(t) \leq V_c(0)$. Therefore, s_f and z are bounded vector functions, and the equilibrium point $(s_f = 0, z = 0)$ of the system (17) and (40) is stable. Because s_f is bounded, s must be bounded. Of course, the boundedness of s implies that $\tilde{\alpha}$ and $\dot{\tilde{\alpha}}$ are bounded. Thus, all the signals in the closed-loop system are bounded. For this reason,

$\ddot{V}_c$ will be bounded. This in turn implies that $\dot{V}_c$ is uniformly continuous. Invoking Barbalat's lemma [25], one can conclude from Eq. (33) that $\dot{V}_c(t)$ tends to zero as $t \to 0$. This implies that s_f , $\phi_f^T z$, and $e = W^T z$ asymptotically converge to zero. Because s_f converges to zero, one finds that s, the tracking error $\tilde{\alpha} = \alpha - \alpha_r$, and its derivative converge to zero as $t \to \infty$. This completes the local asymptotic stability analysis of the generalized closed-loop NCEA system.

Remark 1: The above analysis establishes local asymptotic stability properties of the pitch dynamics. This analysis is valid only if Assumption 2 is satisfied. It is seen in Fig. 3 that the zeros of the transfer function are indeed stable for a set of values of (U, a). Therefore, the trajectories $x(t) = (\alpha(t), h(t), \dot{\alpha}(t), \dot{h}(t))^T$ of the closed-loop system, beginning in the vicinity of $x = 0$, converge to zero. Thus, the derived stability properties of the closed-loop system are valid locally.

Remark 2: Define two manifolds $\mathcal{M}_I$ and $\mathcal{M}_g$ in an extended state space as:

$$\mathcal{M}_I = \{(\phi_f, z) : \phi_f^T z = 0\}$$

$$\mathcal{M}_g = \{(W, z) : W^T z = 0\}$$

Thus, according to the stability analysis, the closed-loop system including the composite identifier has two attractive manifolds $\mathcal{M}_I$ and $\mathcal{M}_g$ to which its trajectories are attracted. Note that NCEA systems have a single attractive manifold, but there does not exist any attractive manifold for CEA systems.

Remark 3: It seen in Eq. (44) that unlike NCEA systems, the derivative of the Lyapunov function includes an additional semi-negative definite function $-\gamma_g (W^T z)^2$. This causes faster decay of V_c. For the NCEA systems, only parameter error dependent semi-negative definite function in $\dot{V}_c$ will be $-(\phi_f^T z)^2$. Of course, in CEA systems, the derivative of Lyapunov functions do not have any z-dependent function.

Now, for the synthesis of the control law, it is necessary to compute the control

input β. Using Eqs. (10), (11), and (16), β can be expressed as:

$$k_f\beta = \dot{\beta}_f + \lambda_f\beta_f = \frac{d}{dt}[-\phi_f^T\hat{\theta}] + \lambda_f\beta_f$$

$$= -\dot{\phi}_f^T\hat{\theta} - \phi_f^T\dot{\hat{\theta}} - \lambda_f\phi_f^T\hat{\theta}$$

$$= -k_f\phi^T\hat{\theta} - \phi_f^T\dot{\hat{\theta}} \tag{45}$$

Using Eqs. (9), (10), (36), and (39), the derivative of $\hat{\theta} = \hat{\theta}_{Igc} + \mu$ can be shown to be:

$$\dot{\hat{\theta}} = \dot{\hat{\theta}}_{Igc} + \dot{\mu}$$

$$= \Gamma[(\lambda_f\phi_f - k_f\phi)s_f + k_1\phi_f s_f - \gamma_g We + \gamma_c\phi_f s_f] + \Gamma[\dot{\phi}_f s_f + \phi_f(-\lambda_f s_f + k_f s)]$$

$$= \Gamma[-\dot{\phi}_f s_f + k_1\phi_f s_f - \gamma_g We + \gamma_c\phi_f s_f] + \Gamma[\dot{\phi}_f s_f + \phi_f(-\lambda_f s_f + k_f s)]$$

$$= \Gamma\phi_f\{(k_1 - \lambda_f)s_f + k_f s\} - \gamma_g\Gamma We + \Gamma\gamma_c\phi_f s_f \tag{46}$$

Finally, substituting $\dot{\hat{\theta}}$ from Eq. (46) in (45) gives the control input β as:

$$k_f\beta = -k_f\phi^T\hat{\theta} - \phi_f^T\Gamma[\phi_f\{(k_1 - \lambda_f)s_f + k_f s\} - \gamma_g We + \gamma_c\phi_f s_f] \tag{47}$$

Note that for this generalized composite NCEA system, γ_c is one.

5 Simulation Results

This section presents the simulation results for the aeroelastic model of Refs. [13, 15]. (Its parameters are collected in the appendix.)

The poles of the linearized system's transfer function for $U = 20m/s$ and $a = -0.6547$ are $1.1975 \pm j13.0787$, $-3.3905 \pm j13.5807$, and the zeros are $-1.6279 \pm j17.5836$ (see Fig. 3). Thus, the open-loop system is unstable, but Assumption 2 holds, and the zero dynamics have locally asymptotically stable equilibrium point. For simulation, the initial conditions chosen are $h(0) = 0.01$ [m], $\alpha(0) = 5$ [deg], $\dot{\alpha}(0) = \dot{h}(0) = 0$.

For the trajectory control, $\alpha_r(t)$ is generated by a fourth-order command generator of the form:

$$(p^2 + 2\rho_1\omega_1 p + \omega_1^2)(p^2 + 2\rho_2\omega_2 p + \omega_2^2)\alpha_r(t) = 0$$

The initial value is $\alpha_r(0) = 5$ [deg], but all of the derivatives of α_r at $t = 0$ are set to zero. The parameters of the command generator are $\rho_1 = \rho_2 = 1, \omega_1 = \omega_2 = 10$. The controller parameters are $\lambda_1 = 15$, $k_1 = 15$, $\lambda_f = 20$, and $k_f = 1$. The initial values of the partial estimates are arbitrarily set as $\hat{\theta}_{Igc}(0) = 0_{9\times1}$. The adaptation gains are $\Gamma = I$, $\gamma_g = \gamma_c = 1$.

***Case A*. Composite NCEA control:** $U = 20$ **m/s,** $a = -0.6547$**,** $(\Gamma, \gamma_g, \gamma_c) = (I, 1, 1)$

First, the closed-loop system for $U = 20m/s$, $a = -0.6547$ is simulated. For a realistic simulation, the maximum value of β has been set to 25^o. The selected responses are shown in Fig. 4. The Figure shows that the pitch angle trajectory smoothly converges to α_r, and the state vector x converges to the origin. We observe oscillatory plunge displacement response. This is because the zero dynamics are underdamped. Additionally, it is seen that along the trajectories of the closed-loop systems, $\phi^T z$ and $W^T z$ are converging to the attractive manifolds $\mathcal{M}_I$ and $\mathcal{M}_g$, respectively.

***Case B*. Composite NCEA control:** $U = 25$ **m/s,** $a = -0.6547$**,** $(\Gamma, \gamma_g, \gamma_c) = (I, 1, 1)$

Next, simulation is done for higher velocity $U = 25$ [m/s] with $a = -0.6547$. The controller used for Case A is retained. Simulated responses are given in Fig. 5. One observes convergence of x to the origin. Due to higher velocity, the control input β waveform is little smoother after the initial saturation, compared with that of Case A. Moreover, the peak values of $\tilde{\alpha}$, $\phi^T z$, and $W^T z$ are smaller, compared with those of Case A, due to increased control effectiveness at higher U.

***Case C*. Composite NCEA control:** $U = 20$ **m/s,** $a = -0.4$**,** $(\Gamma, \gamma_g, \gamma_c) = (I, 1, 1)$

To see the effect of parameter a, simulation is done for $a = -0.4$ with $U = 20$ [m/s]. The controller of Case A is retained. Again, convergence of α and h to zero is observed (see Fig. 6). For this value of a, maximum control input is less than 17 [deg], and maximum $\tilde{\alpha}$ is only 1.5 [deg]. Again, one observes convergence of $\phi_f^T z$ and $W^T z$ to the attractive manifolds $\mathcal{M}_I$ and $\mathcal{M}_g$, respectively.

***Case D.* Composite NCEA control: $U = 25$ m/s, $a = -0.4$, $(\Gamma, \gamma_g, \gamma_c) = (I, 1, 1)$**

Now, simulation is done for $U = 25m/s$, $a = -0.4$ using the controller of Case A. As expected, smoother responses with smaller peak values are observed due to higher velocity $U = 25$ [m/s] (see Fig. 7) compared with those of Case C. The maximum value of β is about 9 [deg] and the maximum plunge displacement is less than 0.015 [m]. Again, $\phi^T z$ and $W^T z$ converge to $\mathcal{M}_I$ and $\mathcal{M}_g$, respectively.

Simulation was done for the other sets of design parameters and adaptation gains. To see the effect on the control magnitude, simulation was done without any imposed limit on the control input β. The performance measures based on the simulated responses (not shown here) are summarized in Tables 1 and 2 for $(\gamma_c = 0, \gamma_g = 0)$, $(\gamma_c = 0, \gamma_g \neq 0)$, $(\gamma_c = 1, \gamma_g = 0)$, and $(\gamma_c = 1, \gamma_g \neq 0)$, but the value Γ is $0.5I$ for Table 1 and $0.2I$ for Table 2, respectively. One observes that for a given value of Γ, the peak values of $\tilde{\alpha}$ and β, and the settling times (denoted as $T_s(\tilde{\alpha})$, $T_s(\phi^T z)$, and $T_s(W^T z)$ for $\tilde{\alpha}$, $\phi_f^T z$, and $W^T z$, respectively), vary with the adaptation gains. It is found that the use of a gradient update rule in the composite identifier reduces the settling time, but a larger control magnitude is required. Additionally, one observes that the closed-loop system with $\gamma_c = 1$ and nonzero γ_g gives improved performance, compared to the controller with ($\gamma_c = 1$, $\gamma_g = 0$), at the cost of a slight increase in β magnitude, as seen in Tables 1 and 2. (One should note that the differences in the response characteristics are small because the LCO is suppressed very quickly, causing lack of excitation in the system.) In the closed-loop system, including the composite identifier with Γ, γ_g, and γ_c all nonzero,

there exist two attractive manifolds $\mathcal{M}_I$ and $\mathcal{M}_g$. Note that NCEA system ($\gamma_g = 0$) will have a single attractive manifold $\mathcal{M}_I$. Of course, there does not exists any attractive manifold for a CEA system ($\gamma_g = 0, \mu = 0$). Moreover, the composite NCEA system including a gradient-based update law has stronger stability properties due to presence of an additional negative semi-definite function ($-|W^T z|^2$) in the Lyapunov derivative (see Eq. (44)). Thus, the use of this generalized composite NCEA control law is preferable.

6 Conclusions

In this paper, the design of an I&I-based generalized composite adaptive control system for the suppression of limit cycle oscillations of a protypical wing section with torsional nonlinearity was considered. The control law was designed based on the choice of the pitch angle treated as a controlled output variable. The control system consisted of a control module and a composite identifier, designed independently. The adaptation law was formed by combining update laws of the NCEA system, classical CEA system, and gradient-based adaptation scheme. The gradient-based update law was formed by an estimation error-based signal, which carries new information on the parameter error. The classical component of the integral update was used to cancel certain sign-indefinite functions in the derivative of the Lyapunov function. Through Lyapunov stability analysis, it was shown that the pitch angle trajectory tracking error and its derivative asymptotically converged to zero. Interestingly, in the closed-loop generalized composite NCEA system, there exist two attractive manifolds to which the system's trajectories converged. This does not happen in classical certainty-equivalence and also in noncertainty-equivalence adaptive systems. Simulation results were obtained, which showed the suppression of limit cycle oscillations and convergence of the state vector to the origin, despite uncertainties in the model parameters. Furthermore, it was found that the composite NCEA control law, including the update rules of the CEA system and the gradient scheme, provides superior performance in the closed-loop system, compared

with the NCEA system.

Appendix

1. System Parameters

$b = 0.135$[m], $m_w = 2.049$[kg], $c_h = 27.43$[Ns/m], $c_\alpha = 0.036$[Ns]

$\rho = 1.225$[kg/m^3], $c_{l\alpha} = 6.28, c_{l\beta} = 3.358, c_{m\alpha} = (0.5 + a)c_{l\alpha}$

$c_{m\beta} = -0.635, m_t = 12.387$[kg], $I_\alpha = 0.0517 + m_w x_\alpha^2 b^2$ [kg $\cdot$ m^2]

$x_\alpha = [0.0873 - (b + ab)]/b$

$k_\alpha = 2.82 * (1 - 22.1\alpha + 1315.5\alpha^2 - 8580\alpha^3 + 17289.7\alpha^4)$[N $\cdot$ m/rad]

$k_{h0} = 2844.4$[N/m]

2. Performance characteristics as functions of the adaptation gains γ_g and γ_c

Table 1: The effect of (γ_g, γ_c) on the performance of the composite law; $a = -0.6547, U = 20$[m/s], $\omega_1 = \omega_2 = 2, k_1 = \lambda_1 = 15, \lambda_f = 20, k_f = 1, \Gamma = 0.5I$, $T_s(\tilde{\alpha})$(Settling time), $T_s(\phi_f^T z)$(Settling time), $T_s(W^T z)$(Settling time)

Type	max($\lvert\tilde{\alpha}\rvert$)[deg]	$T_s(\tilde{\alpha})$ [sec]	max($\lvert u\rvert$)[deg]	$T_s(\phi_f^T z)$[sec]	$T_s(W^T z)$[sec]
$\gamma_c = 0, \gamma_g = 0$	2.5009	2.9370	33.0197	2.2470	-
$\gamma_c = 0, \gamma_g = 1$	2.5089	2.9350	33.0129	2.2460	2.6820
$\gamma_c = 1, \gamma_g = 0$	2.4761	2.9240	33.4339	2.2320	-
$\gamma_c = 1, \gamma_g = 1$	2.4839	2.9220	33.4199	2.2310	2.6800
$\gamma_c = 1, \gamma_g = 5$	2.5145	2.9130	33.4045	2.2250	2.6860

Disclosure of potential conflicts of interest - ethical and financial

Conflict of Interest: The authors declare that they have no conflict of interest.

Table 2: The effect of (γ_g, γ_c) on the performance of the composite law; $a = -0.6547, U = 20$[m/s], $\omega_1 = \omega_2 = 2, k_1 = \lambda_1 = 15, \lambda_f = 20, k_f = 1$, smaller $\Gamma = 0.2I$, $T_s(\tilde{\alpha})$(Settling time), $T_s(\phi_f^T z)$(Settling time),$T_s(W^T z)$(Settling time)

Type	max($\lvert\tilde{\alpha}\rvert$)[deg]	$T_s(\tilde{\alpha})$ [sec]	max($\lvert u\rvert$)[deg]	$T_s(\phi_f^T z)$[sec]	$T_s(W^T z)$[sec]
$\gamma_c = 0, \gamma_g = 0$	3.3350	2.9870	27.8759	2.3800	-
$\gamma_c = 0, \gamma_g = 1$	3.3391	2.9860	27.8837	2.3780	2.6150
$\gamma_c = 1, \gamma_g = 0$	3.3015	2.9760	28.2799	2.3570	-
$\gamma_c = 1, \gamma_g = 1$	3.3055	2.9750	28.2847	2.3560	2.6200
$\gamma_c = 0, \gamma_g = 10$	3.3757	2.9790	27.9606	2.3680	2.6150
$\gamma_c = 1, \gamma_g = 10$	3.3415	2.9670	28.3768	2.3470	2.6190

References

1. Lee, B. H. K., Price, S. J., and Wong, Y. S., "Nonlinear Aeroelastic Analysis of Airfoils: Bifurcation and Chaos," *Progress in Aerospace Sciences*, Vol. 35, No. 3, 1999, pp. 205-334. doi:10.1016/S0376-0421(98)00015-3

2. Thomas, J. P., Dowell, E. H., and Hall, K. C.,"Nonlinear Inviscid Aerodynamic Effects on Transonic Divergence, Flutter, and Limit-Cycle Oscillations," *AIAA Journal*, Vol. 40, No. 4, 2002, pp. 638-646.

3. Gilliatt, H. C., Strganac, T.W., and Kurdila, A. J., "An Investigation of Internal Resonance in Aeroelastic Systems," *Nonlinear Dynamics*, Vol. 31, No. 1, 2003, pp. 1-22. doi:10.1023/A:1022174909705

4. Marzocca, P., Librescu, L., and Silva, W. A.,"Flutter, Postflutter, and Control of a Supersonic Wing Section," *Journal of Guidance, Control, and Dynamics*, Vol. 25, No. 5, 2002, pp. 962-970.

5. Mukhopadhyay, V., "Historical Perspective on Analysis and Control of Aeroelastic Responses," *Journal of Guidance, Control, and Dynamics*, Vol. 26, No. 5, 2003, pp. 673-684.

6. Waszak, M. R., "Robust Multivariable Flutter Suppression for Benchmark Active Control Technology Wind-Tunnel Model," *Journal of Guidance, Control, and Dynamics*, Vol. 24, No. 1, 2001, pp. 147-153.

7. Mukhopadhyay, V., "Transonic Flutter Suppression Control Law Design and Wind-Tunnel Test Results," *Journal of Guidance, Control and Dynamics*, Vol. 23, No. 5, 2000, pp. 930-937.

8. Kelkar, A. G., and Joshi, S. M., "Passivity-Based Robust Control with Application to Benchmark Controls Technology Wing," *Journal of Guidance, Control and Dynamics*, Vol. 23, No. 5, 2000, pp. 938-947.

9. Barker, J. M., and Balas, G. J., "Comparing Linear Parameter- Varying Gain Scheduled Control Techniques for Active Flutter Suppression," *Journal of Guidance, Control and Dynamics*, vol. 23, no. 5, 2000, pp. 948-955.

10. D. M. Guillot and P. P. Friedmann, "Fundamental aeroservoelastic study combining unsteady computational fluid mechanics with adaptive control," *Journal of Guidance, Control and Dynamics*, vol. 23, no. 6, pp. 1117-1126, 2000.

11. Scott R. C., and Pado, L. E., "Active control of wind-tunnel model aeroelastic response using neural networks," *Journal of Guidance, Control and Dynamics*, vol. 23, no. 6, 2000, pp. 1100-1108.

12. Shukla, H., Patil, M. J.: Nonlinear state feedback control design to eliminate subcritical limit cycle oscillations in aeroelastic systems. Nonlinear Dyn. 88, 15991614 (2017)

13. Ko, J., Kurdila, A. J., and Strganac, T. W., "Nonlinear Control of a Prototypical Wing Section with Torsional Nonlinearity," *Journal of Guidance, Control and Dynamics*, Vol. 20, No. 6, 1997, pp. 1181-1189.

14. Sheta, E. F., Harrand, V. J., Thompson, D. E., and Strganac, T. W., " Computational and Experimental Investigation of Limit Cycle Oscillations of Nonlinear Aeroelastic Systems," *Journal of Aircraft*, Vol. 39, No. 1, 2002, pp. 133-141.

15. Block, J. J., and Strganac, T. W., "Applied Active Control for a Nonlinear Aeroelastic Structure," *Journal of Guidance, Control, and Dynamics*, Vol. 21, No. 6, 1998, pp. 838-845.

16. Platanitis, G., and Strganac, T. W.,"Control of a Nonlinear Wing Section Using Leading- and Trailing-Edge Surfaces," *Journal of Guidance, Control, and Dynamics*, Vol. 27, No. 1, 2004, pp. 52-58.

17. Xing, W., and Singh, S. N.," Adaptive Output Feedback Control of a Nonlinear Aeroelastic Structure," *Journal of Guidance, Control and Dynamics*, Vol. 23, No. 6, 2000, pp. 1109-1116.

18. Behal A., Marzocca, P., Rao, V. M., and Gnann, A.," Nonlinear Adaptive Control of an Aeroelastic Two-Dimensional Lifting Surface," *Journal of Guidance, Control, and Dynamics*, Vol.29 No.2, 2006, pp. 382-390.

19. Gujjula, S, Singh, S. N., and Yim, W., "Adaptive and Neural Control of a Wing Section Using Leading- and Trailing-Edge Surfaces," *Aerospace Science and Technology*, Vol. 9, No. 2, 2005, pp. 161-171.

20. Behal, A., Rao, V. M., Marzocca, P., and Kamaludeen, M.," Adaptive Control for a Nonlinear Wing Section with Multiple Flaps ," *Journal of Guidance, Control, and Dynamics*, Vol 29, No. 3, 2006, pp. 744-749.

21. Reddy, K. K., Chen, J., Behal, A., and Marzocca, P.," Multi-Input/Multi-Output Adaptive Output Feedback Control Design for Aeroelastic Vibration Suppression," *Journal of Guidance, Control, and Dynamics*, Vol. 30, No. 4, 2007, pp. 1040-1048.

22. Lee, K.W., and Singh, S. N.,“ L_1 Adaptive Control of a Nonlinear Aeroelastic System Despite Gust Load,” *Journal of Vibration and Control*, Vol. 19, No. 12, 2013, pp. 1807-1821.

23. Zhang, K., Wang, Z., Behal, A., and Marzocca,“Novel Nonlinear Control Design for a Two-Dimensional Airfoil Under Unsteady Flow,” *Journal of Guidance, Control, and Dynamics*, Vol. 36, No. 6, 2013, pp. 1681-1694.

24. Wang, Z., Behal, A., and Marzocca, P., “ Model-Free Control Design for Multi-Input Multi-Output Aeroelastic System Subject to External Disturbance,” *Journal of Guidance, Control, and Dynamics*, Vol. 34, No. 2, 2011, pp. 446-458.

25. Chen, C.L., Chang, C.W, Yau, H.T.: Terminal sliding mode control for aeroelastic systems. Nonlinear Dyn. 70, 2015-2026 (2012)

26. Ioannou, P. A., and Sun, J., Stable and Robust Adaptive Control, Prentice-Hall, Upper Saddle River, NJ, 1995, pp. 85-134.

27. Astolfi, A., Karagiannis, D., and Ortega, R., Nonlinear and Adaptive Control with Applications, SpringerVerlag, London, 2008, pp. 276-309.

28. Seo, D., and Akella, M. R., “High-Performance Spacecraft Attitude- Tracking Control Through Attracting-Manifold Design,” *Journal of Guidance, Control, and Dynamics*, Vol. 31, No. 4, 2008, pp. 884891. doi:10.2514/1.33308

29. Lee, K. W., Singh, S. N.: Non-certainty-equivalence adaptive control of a nonlinear aeroelastic system. Intl J. of Electronics and Telecommunications. 56, 463-471 (2010)

30. Lee, K. W., and Singh, S. N., “Multi-Input Noncertainty-Equivalent Adaptive Control of an Aeroelastic System,” *Journal of Guidance, Control, and Dynamics*, Vol. 33, No. 5, 2010, pp. 1451-1460. doi:10.2514/1.48302

31. Mannarino, A., and Mantegazza, P., "Multifidelity Control of Aeroelastic Systems: An Immersion and Invariance Approach," *Journal of Guidance, Control, and Dynamics*, Vol. 37, No. 5, 2014, pp. 1568-1582.

32. Duarte, M. A., Narendra, K. S., "Combined direct and indirect approach to adaptive control," *IEEE. Trans. Autom. Control*, Vol. 34, No.10, 1989, pp. 1071-1075.

33. Slotine, J.-J. E., Li, W., "Composite adaptive control of robot manipulators," *Automatica* Vol. 25, No. 4, 1989, pp. 509-519.

34. Patre, P. M., Bhasin, S., Wilcox, Z. D., Dixon, W. E., "Composite adaptation for neural network-based controllers," *IEEE Trans. Autom. Control*, Vol. 55, No.4, 2010, pp. 944-950.

35. Lavretsky, E.,"Combined/composite model reference adaptive control," *IEEE Trans. Autom. Control*, Vol. 54, No. 11, 2009, pp. 2692-2697.

36. Liu, Z., Yuan, R., Fan, G., Yi, J., "Immersion and invariance based composite adaptive control of nonlinear high-order systems," *Proceedings of 2018 Chinese Control and Decision Conf.*, IEEE, 2018, pp. 96-101.

37. Lee, K. W., Singh, S. N.," Generalized Composite Noncertainty-Equivalence Adaptive Control of Orbiting Spacecraft in Vicinity of Asteroid," *Journal of Astronautical Sciences*, 2020.

38. Ioannou, P. A., and Sun, J., Stable and Robust Adaptive Control, Prentice-Hall, Upper Saddle River, NJ, 1995, pp. 85-134.

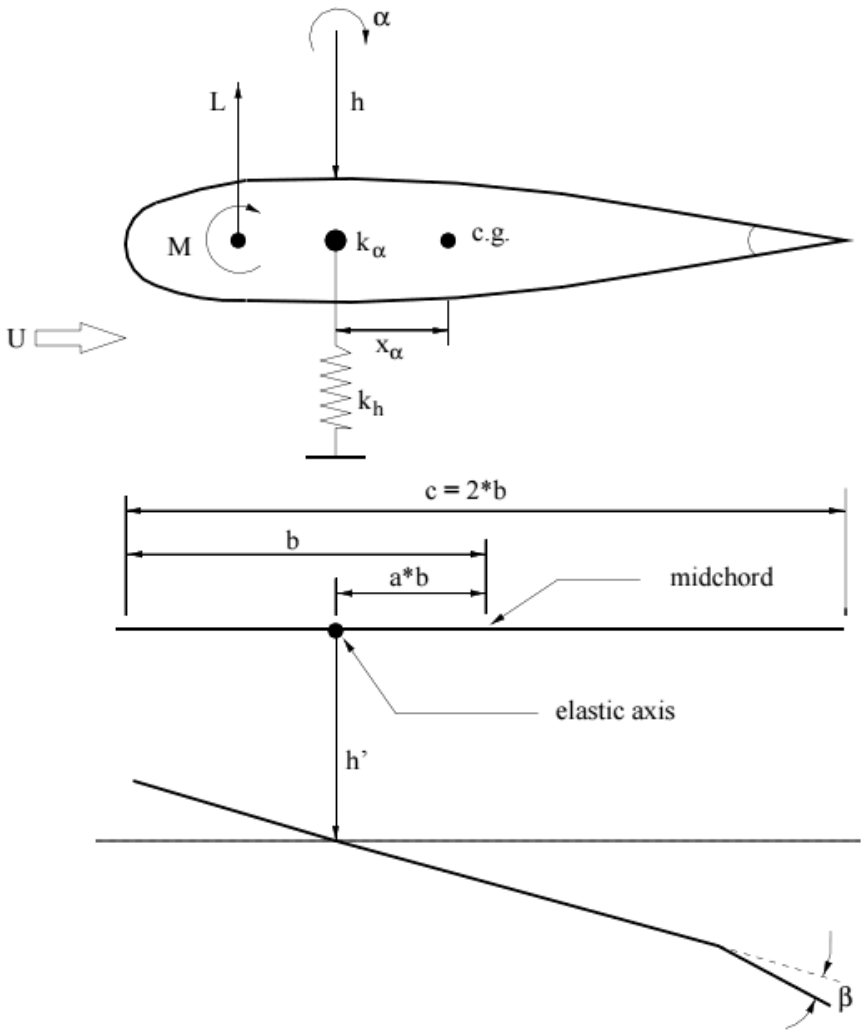

Figure 1: Aeroelastic system with trailing-edge control surface

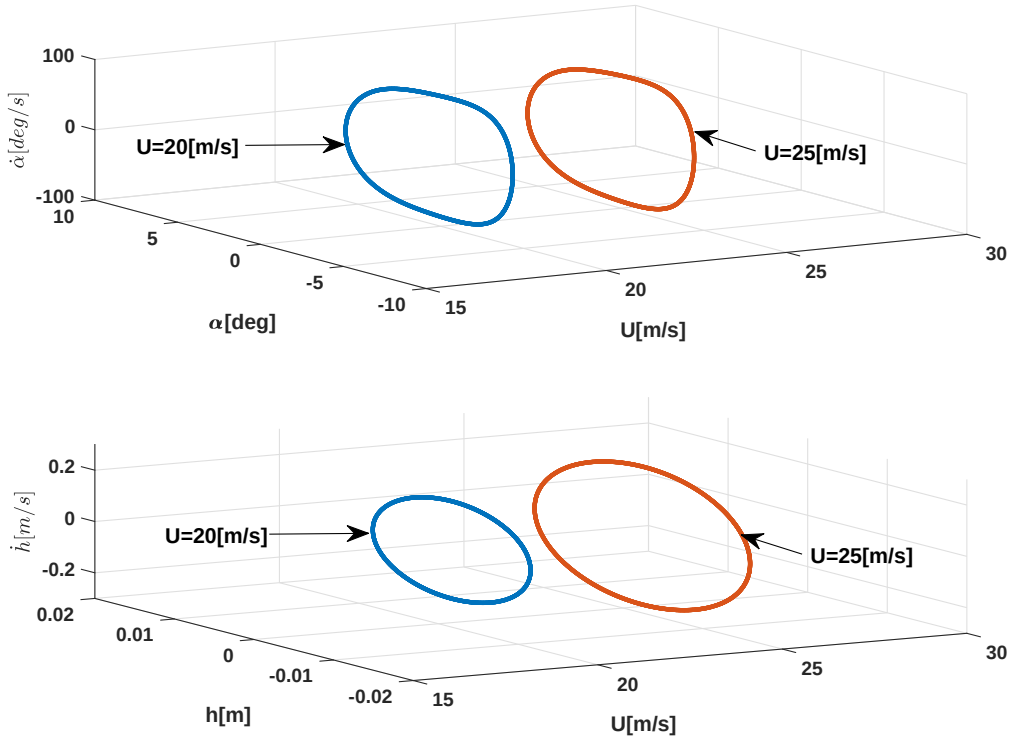

Figure 2: Limit cycles in the phase-planes for $U = 20$ and 25 [m/s], $a = -0.6547$

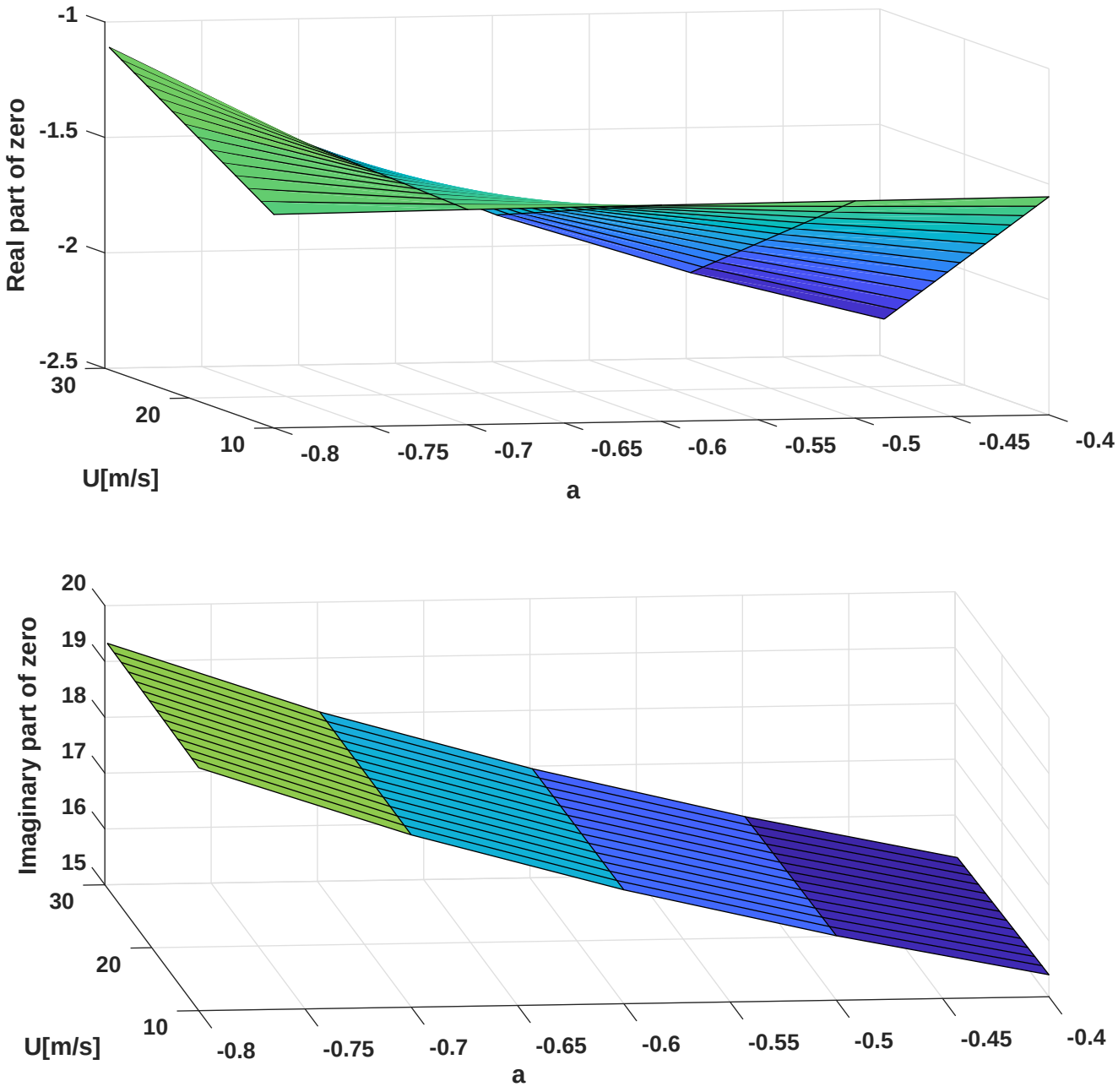

Figure 3: Real and positive imaginary parts of zeros of the transfer function

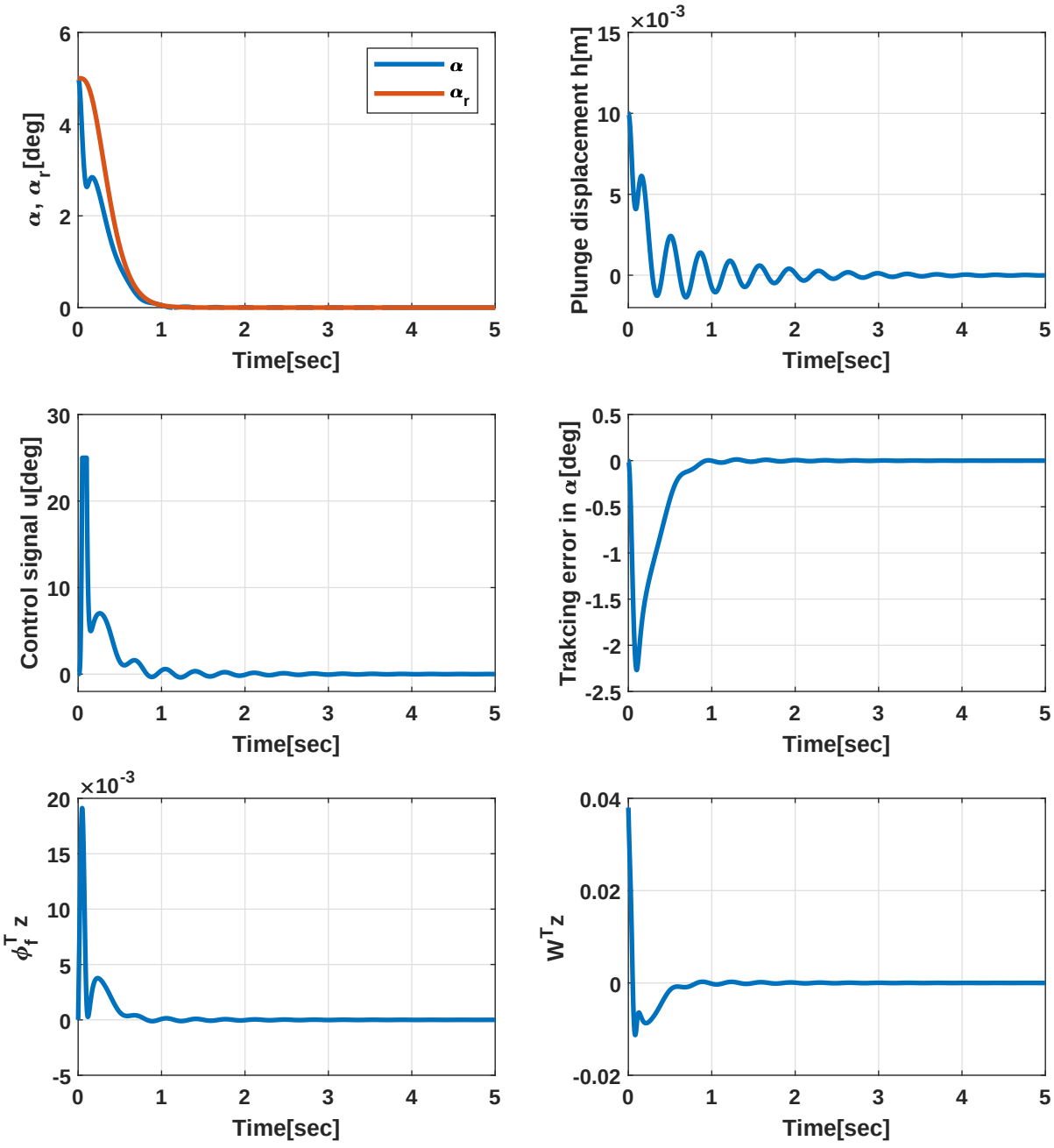

Figure 4: Composite NCEA control: $U = 20$ [m/s], $a = -0.6547$, $\Gamma = I$, $\gamma_g = \gamma_c = 1$

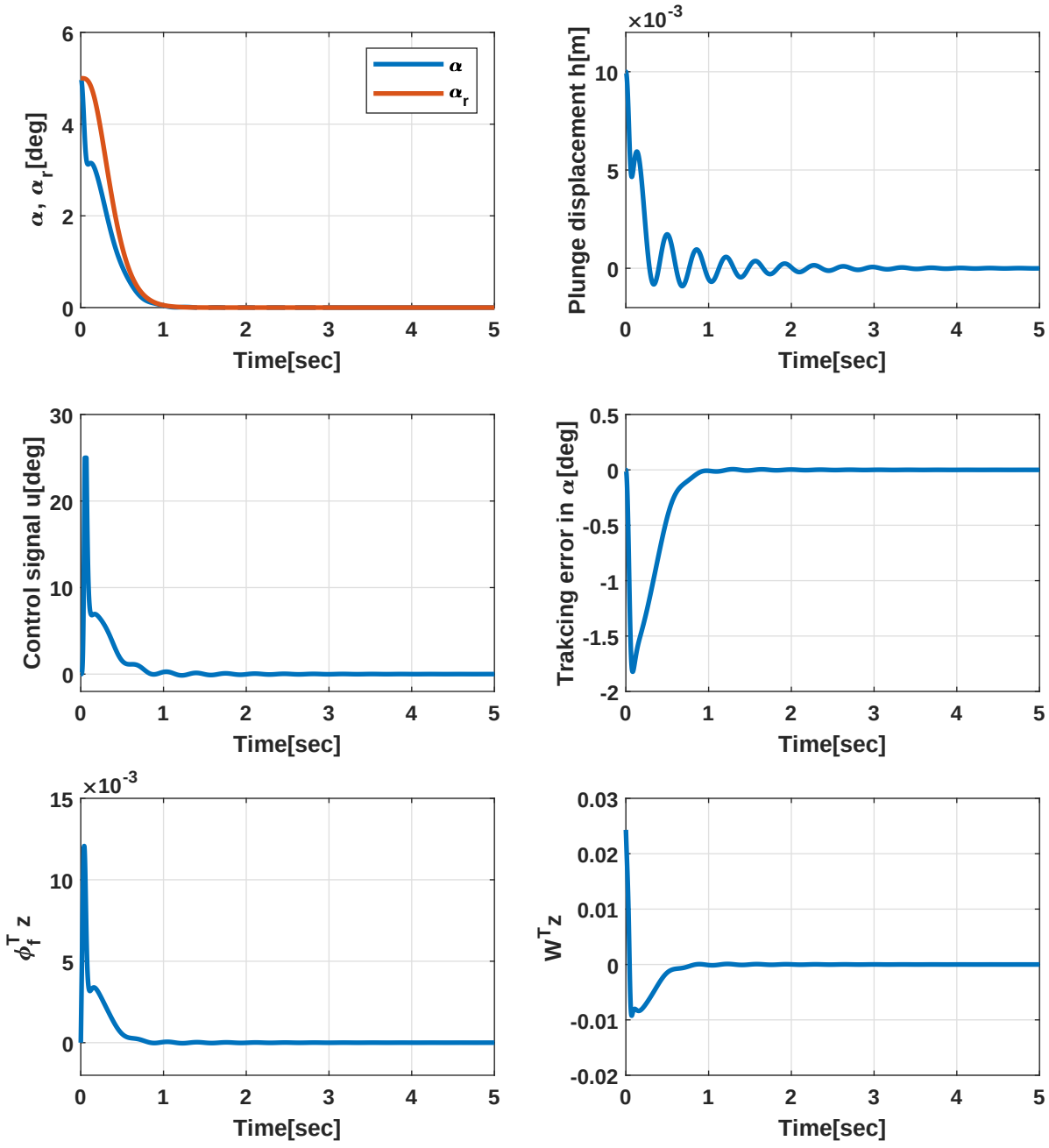

Figure 5: Composite NCEA control: $U = 25$ [m/s], $a = -0.6547$, $\Gamma = I$, $\gamma_g = \gamma_c = 1$

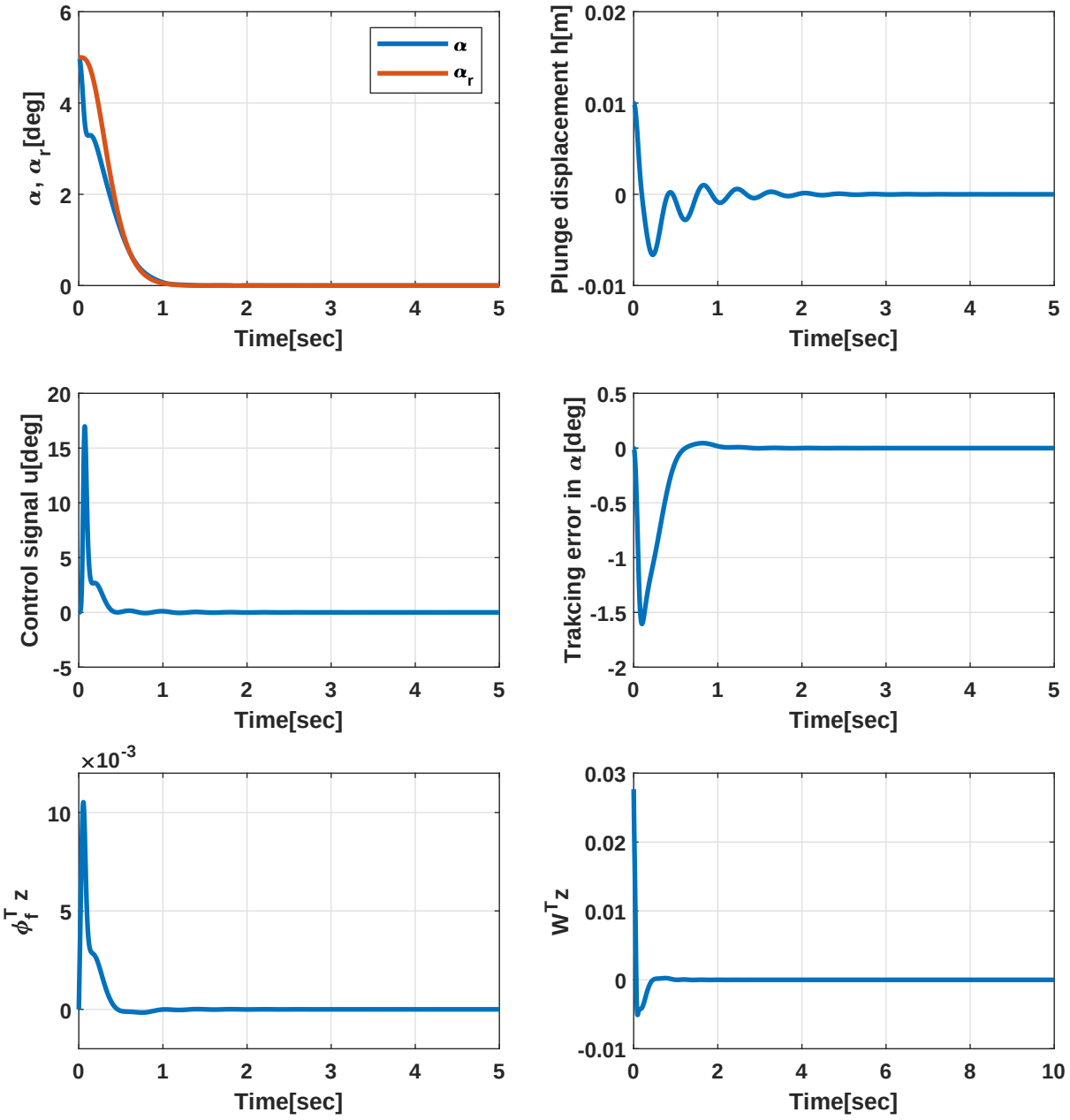

Figure 6: Composite NCEA control: $U = 20$ [m/s], $a = -0.4$, $\Gamma = I$, $\gamma_g = \gamma_c = 1$

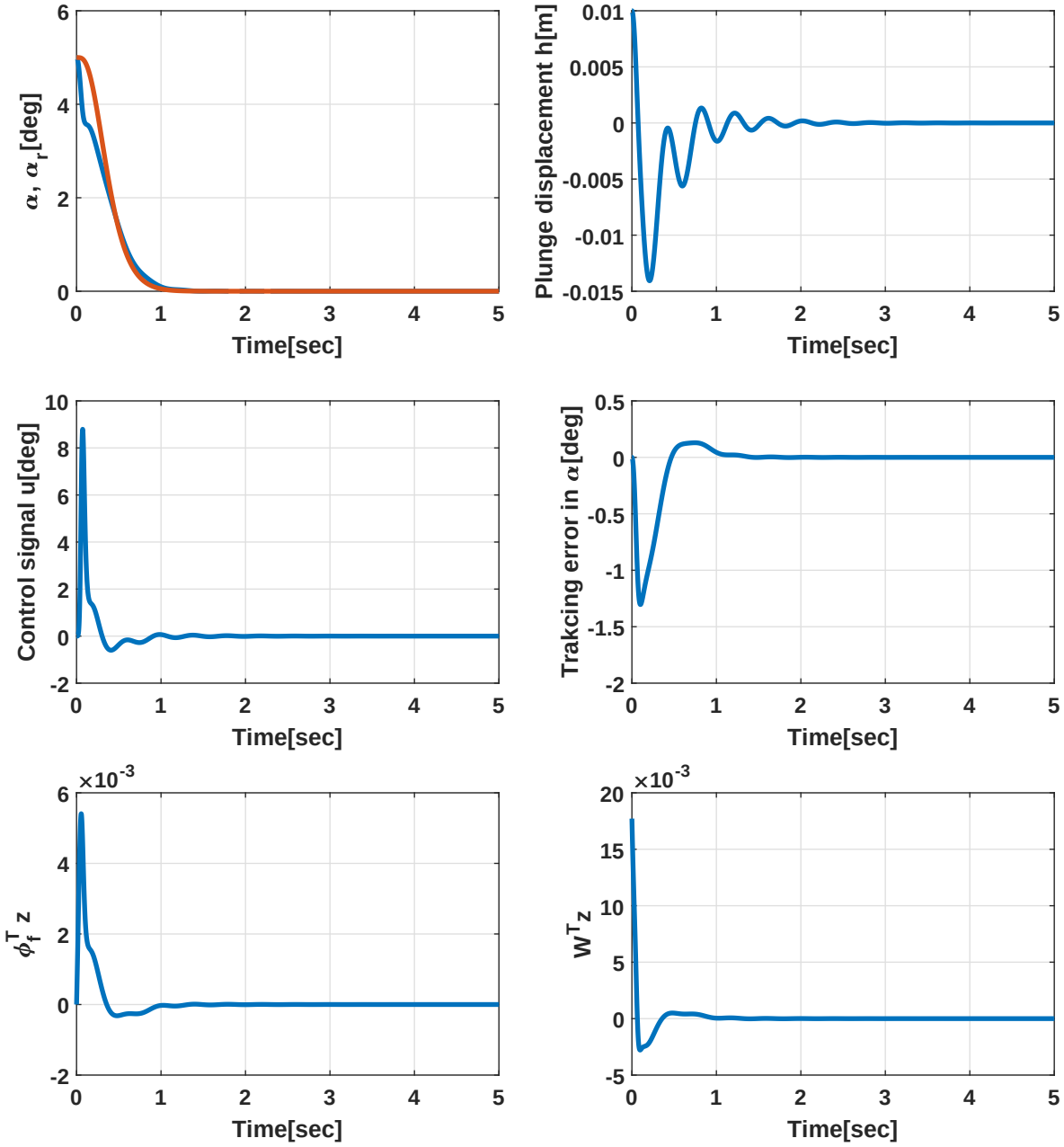

Figure 7: Composite NCEA control: $U = 25$ [m/s], $a = -4$, $\Gamma = I$, $\gamma_g = \gamma_c = 1$